Geopersia ***10*** *(2), 2020, PP. 333-349* *DOI: 10.22059/GEOPE.2020.287814.648497*

Studying Evolutionary Processes of Petergan Playa Brines in South Khorasan, East of Iran

Hengameh Erfanian Kaseb[1], Habib Allah Torshizian[2]*, Davod Jahani[1], Mohammad Javanbakht[2], Nader Kohansal Ghadimvand[1]

[1] *Department of Geology,Islamic Azad University, North Tehran Branch, Tehran, Iran*

[2] *Department of Geology, Islamic Azad University, Mashhad Branch, Mashhad Iran*

**Corresponding author, e–mail: habib.torshiziyan@gmail.com*

(*received: 25/08/2019 ; accepted: 26/01/2020*)

Abstract

The Petergan Playa lies in east of Iran, covering an area of 212.5 km^2. The playa is located 135 km from the city of Qayen, South Khorasan Province, Iran at the border area known as Shahrakht. Some parts of the playa have stretched into Afghanistan. Thus, the present research was conducted to study the brines and their evolution, sampling was done from some of 95 brines based on an ordered network, and their location was spotted by the GPS. Depth and status of sampling were also recorded. The brines were analyzed using the Inductively Coupled Plasma–Mass Spectrometry (ICP–MS) method. The cations found in the brines showed an abundance in the amounts of Na^+,Ca^{2+}, Mg^{2+}, and K^+. For the anions, an abundance was observed in the amounts of Cl^-, SO_4^{2-}, and HCO_3^-. The type of brines was as follows: Na^+, $-SO_4^{2-}$, and $-Cl^-$. By pondering about fairly neutral acidity and chemical investigation of the ingress waters, it was inferred that, the waters are of $Ca^{2+} > CO_3^{2-}$, $Cl^- + SO_4^{2-} > HCO_3^-$, $HCO_3^- \ll Ca^{2+} + Mg^{2+}$ molar ratios, that follows the geochemical route Π in the brines' geochemical evolution diagram, which is similar to the brines present in Saline Valley and the Dead Valley in the United States. X–Ray Diffraction (XRD) results revealed that, the most abundant minerals in the brines are Quartz, Gypsum, Halite, and Calcite, while the least abundant minerals are Muscovite, Clinochlore, and Albite. Accordingly, source of the brines would be meteoric waters as well as neutral waters and brines with hydrothermal source.

Keywords: *Playa, Dead Valley, East of Iran, Hydrogeochemistry, Brine Evolution.*

Introduction

Not only in Iran, but also around the world, history of studies carried out on brine lakes and playa is not long–standing. Notwithstanding, numerous studies have been carried out in this regard including the study on evaporative depositions (Hardie, 1968), evolution of brines in confined basins (Ma *et al.,* 2010), mineralogy and geochemical evolution of evaporate lakes (Bahadory *et al.,* 2011; Lee *et al.,* 2013) .There are studies on playa deposits in regional scale in Kuwait (Al–Dousari, 2005; Ahmed *et al.,* 2016). Study on the playa is important due to the fact that, playa acts as ecological system that should be maintained. Also, playa deposits act as a source of dust (Al–Dousari & Al–Hazza, 2013; Al–Dousari, 2009; Al–Dousari *et al.,* 2016) and radionuclides in the area (Aba *et al.,* 2016; Aba *et al.,* 2018). A worker named Krinsley has also studied the Iranian playa (1970) regarding its geomorphology and palaeoclimatology. Conflating the data related to 2 disparate time zones (1975–2002, summer 2002, and spring 2005), Fayazi *et al.* (2007) have studied brine evolution of the Lake Maharlou. Their results were comparable to those of the study on American salt lakes. Lak *et al.* (2016) investigated hydrogeochemistry characteristics and determined the source and evolution of brines of the Howz–e–Soltan Lake in Qom. Abdi & Rahimpour Bonaab (2010) conducted surveys on hydrogeochemical characteristics and brine evolution of the Meyghan Playa in Arak. Torshizian & MusaviHarami (1999) assessed sedimentology, geochemistry, and hydrogeochemistry phenomena of the Zarrin Playa in Central Iran. Torshizian *et al.* (2009) investigated brine evolution and formation of evaporate minerals in the Saghand Playa in Central Iran, and they drew an analogy with the Great Salt Lake and the Basin of Dead Valley in the States. A team of workers have (2006) also conducted an analysis on hydrogeochemical characteristics of playa brine of the Siyah–Kuh Mountain in Central Iran. Thus, the present study was conducted to determine source of hydrogeochemical evolution of Petergan Playa brines lying in northeast of the country. To do so, the outcrops around the playa and geology of the area were taken into account aimed at finding a relevant relationship between hydrogeochemical characteristics of the brines and the type of outcrop.

Methodology

The Petergan Playa lies in east of Iran, locating 135

km from the city of Qayen, South Khorasan Province, Iran in a border region called Shahrakht, at coordination of E 60°30′ to 60°56′ and N 33°10′ to 33°30′. The playa is 610 m above the sea level, with 30 km width, and 50 km length (altogether with the section stretched into Afghan mainland) (see Fig. 1).

Initially, a virtually ordered square–shaped sampling method was designed with the profiles trending of N–S at intervals of 1 km in an area of 172 km^2 (see Fig. 2). A total of 103 test pits of 2–4 m depth were dug to provide a better access to subterranean brines, out of which 95 ones hit the target and 8 ones did not. Sampling procedure was performed in October and November from margins of playa towards the center along the profiles. Using the GPS during sampling, some data such as depth, coordination, and route of the sampling were obtained and recorded on sampling cards. Then, the samples were stored in 1.5 L polyethylene containers and were labeled. Later on, the samples were sent to the laboratory for ICP–MS analysis and identification of mineralogical characteristics of some sediment taken from the test pits, the former were analyzed using the XRD. The analyses were conducted in the laboratories of the Iranian Mines & Mining Industries Development & Renovation (IMIDRO) company located in Karaj, Alborz Province and the *Zarazma* Mineral studies Company, located in Tehran, Tehran Province, Iran. Besides the ICP analysis, other methods were applied, which were as follows: The silver nitrate method was applied to measure cations and anions, the alkalinity method was used to determine bicarbonate amount, and the opacity method was applied to measure amount of sulfate. Authenticity of the laboratory results was checked using recurring samples, and precision of the analyses was checked by representative samples. Ultimately, to analyze the content of the Petergan Playa brines, the Rock Work was used, to determine chemical composition, Piper triangular diagrams were used according to the study by Hardie (1970), and to measure average density of elements, Stiff diagrams were employed.

Geology of the Study Area

Conflating the 1:250000 maps of the Shahrakht (Fauvelet & Eftekhar Nezhad, 1990) with the 1:250000 map of Herat (Williams, 2005) in the GIS suite, a comprehensive map of 1:650000 was prepared (see Fig. 3).

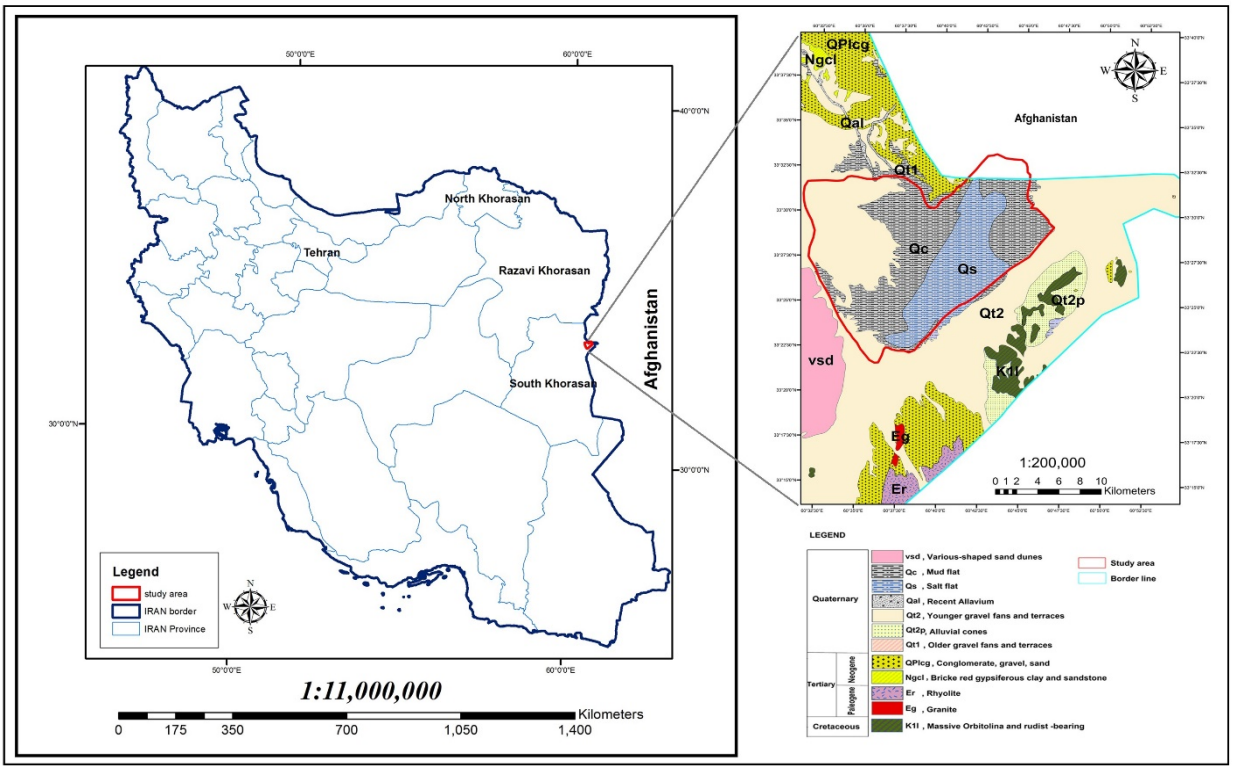

Figure 1. The location of the Petergan Playa along/ at the eastern border line.

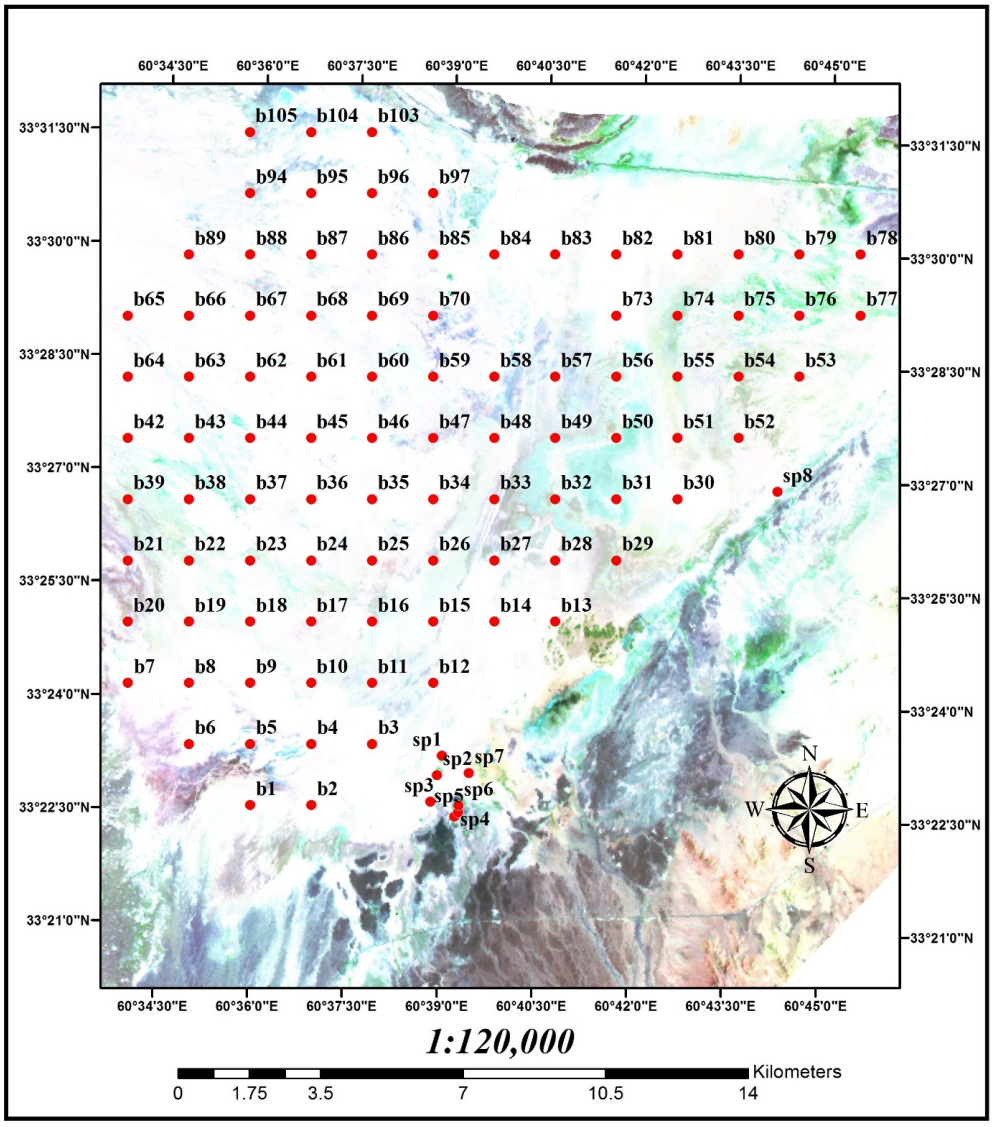

Figure 2. The sampling network designed for the Petergan Playa brines.

Based on the classification offered by Jones & Deocampo (2014), formation and lithology of the rocks surrounding the basin were classified into 7 kinds: evaporites, pyroclastics, carbonates, mafic silicates, plagioclase feldspars, calcites and sulphides, silicates, and sulphides, all displaying a coherent relationship between hydrogeochemical characteristics of the brines and type of the outcrops around the playa.

The Petergan Playa was buried by clayey soils. Main share of the area was covered by Quaternary deposits, in the west by Pliocene conglomerate and basalts, and in the east by Aeolian deposits, ancient and juvenile terraces, clay, and desert flats (Fig. 6(a)). The most prominent outcrops included orbitolina massive limestones, sandstone, clay, shale, and conglomerate with a red and Fe–bearing cement of Lower Cretaceous (Fig.6 (b),(c)) based on the 1:650000 conflated map of Shahrakht–Herat along with systematic geochemical studies related to 1:100000 map of Shahrakht and Yazdaan (Sa'deddin *et al.,* 2006).

The outcrops were found to be associated with some metamorphic units, intermediate–acidic igneous rocks, and basic igneous rocks of Palaeogene, Neogene, and Quaternary together with negligible volumes of calcareous and dolomitic carbonate rocks (Fig. 6 (g)). Remarkable part of the area was covered by depositional alluvium, salt, muddy, and sandy flats, as well as running sands

(Fig. 6 (d, e), and (f)).

As illustrated on the 1:650000 lithology map of Shahrakht–Herat (Fig. 4), the most abundant rock units in terms of abundance percentage are silicates and sulphides of 79% widespread at entire directions, plagioclase feldspars of 12%, showing the most massive distribution in the southeast, and carbonates of 4.7% and mafic silicates of 1.9% distributed in the southeast of the area. Remaining rocks are evaporate outcrops of 1.6% lying in northwest of the playa, calcites and sulphides of 0.4% in northwest, and ultimately the pyroclastics of a meager ratio of 0.1% in west (see Fig. 5).

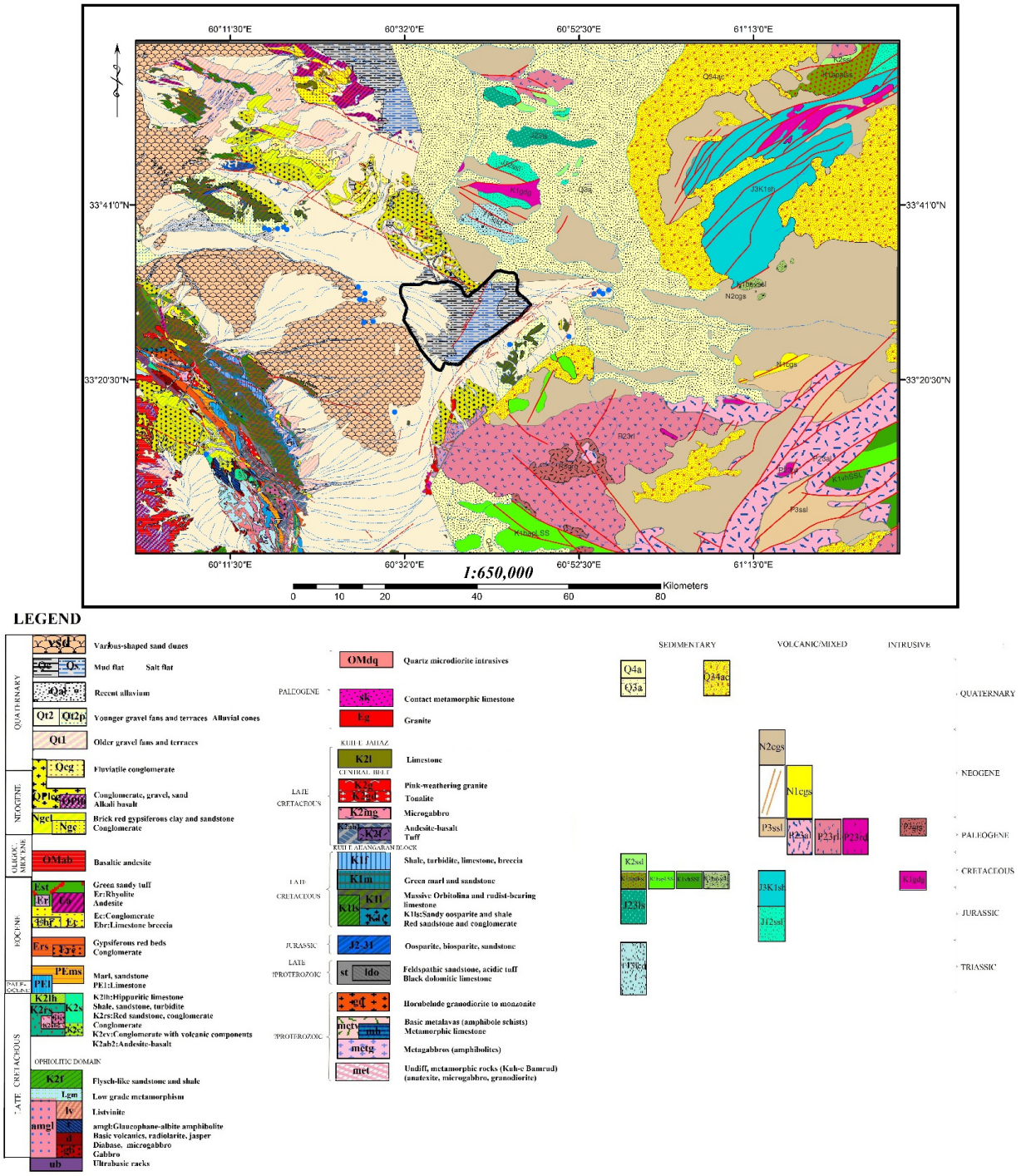

Figure 3. The 1:650000 conflated geology map of Shahrakht–Herat (Williams, 2005; Fauvelet & Eftekhar Nezhad, 1990).

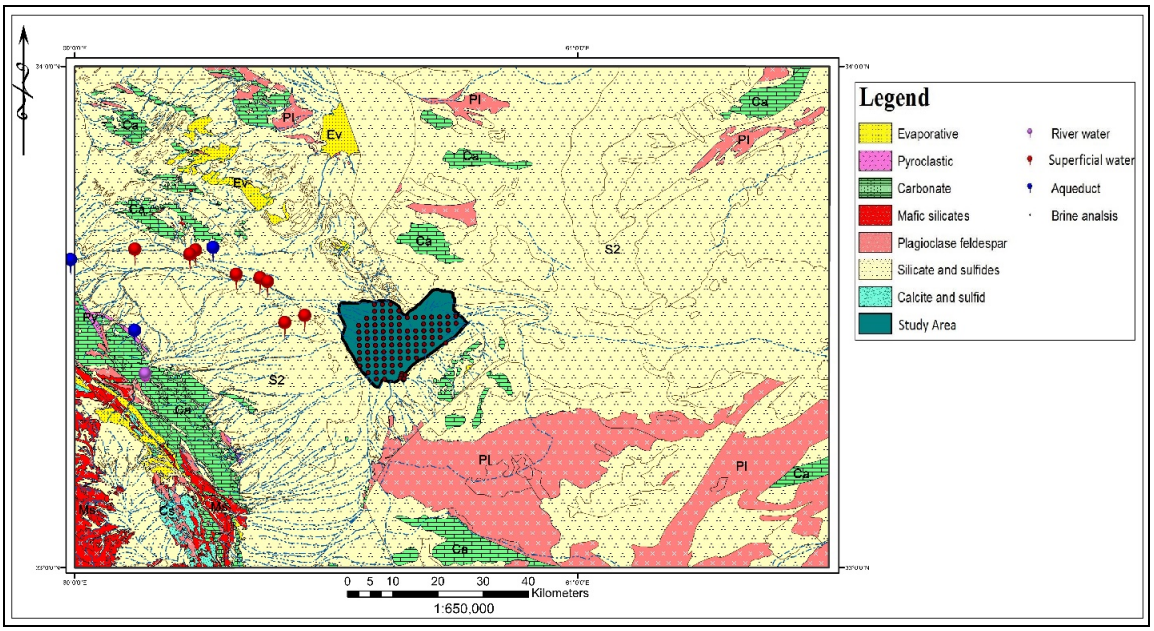

Figure 4. The 1:650000 lithology map of the rocks surrounding the Petergan Playa.

Results Obtained from Analysis of the Water and Brine

Hydrogeochemical composition of the brines relies on their present salts carried in ingress waters, meteoric waters, and chemical weathering of rocks, and also basin´s sediments (Eugester & Hardie, 1978). Hence, there is a direct relationship between the content of salts and the lithology of the watershed and newly formed rocks by the salts, cations, and anions carried by ingress waters.

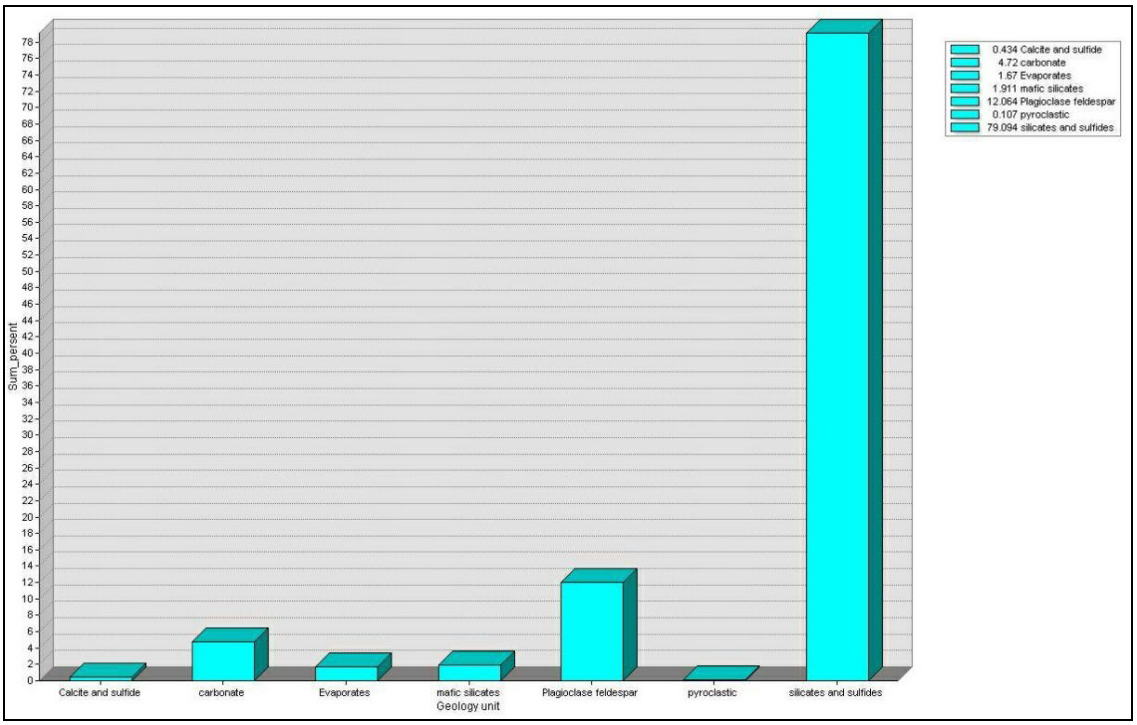

Figure 5. The stretch of rock units around the Petergan Playa based on the lithology map of 1:650000 of Shahrakht–Herat.

In fact, knowing about formulation of $Ca^{2+} + Mg^{2+} / HCO_3^-$ plays a pivotal role in determination of evolutionary route of the brines (Jones & Deocampo, 2014). The data obtained from all chemical analyses were assessed in order to investigate hydrogeochemical characteristics of the brines and their evolution (see Table 1). Results showed that, for the brines, acidity rate of 5.8–8 is slightly acidic to slightly alkaline. Electric Conductivity (EC) of the brines varied between 7.57–547 mS/cm and rate of total hardness was equal to 84.5 mg/L.

The most abundant cations were sodium, calcium, magnesium, potassium, and the most abundant anions were chloride, sulfate, and bicarbonate, respectively. The brines are generally rich in sodium, chlorine, and sulfate while possessing the meager amounts of other minerals such as calcium, magnesium, potassium, and bicarbonate. Average amount for the minerals was measured as 45319.4 Na^+, 1498.1 Ca^{2+}, 1498.6 Mg^{2+}, 177.1 K^+, 70400 Cl^-, 5500 SO_4^{2-}, and 80 (ppm) HCO_3^-. Na^+ had the greatest concentration in ingress water i.e., qanats, rivers (surface waters) and wells, concentration of Na^+ was equal to 10.98, 24.50 ,and 8.9 in surface waters, wells ,and qanats, respectively. However, the lowest concentration of cations was related to K^+ by 0.01 for surface waters and qanats and by 0.04 for wells, on average, Cl^- had the greatest concentration among the anions by 6.80, 6.65, and 20.95 as measured in surface waters (rivers, qanats) and wells, while the lowest concentration was related to CO_3^{2-} by 0.01. The increase in the concentration of anions and cations towards the center of the basin results from the analogy drawn between chemical analysis results of the brines with those of the ingress waters.

The diagrams of Piper and Stiff were employed to investigate chemical events of the brines. The principle anions stand on 3 apexes of a triangle and cations on 3 apexes of contiguous triangle, and chemical content of each stripe of water was determined based on percentage of cations and anions resting on the diagram in the form of an individual point. Chemical content and the relationship between vaudeville watersheds can be understood solely by a brief glance at the diagram. Chemical content of waters in the watersheds and, as a result, chemical content of ingress waters to the playa was variegated consisting of chlorurea, sulfate ,and carbonate (mostly chlorurea), whereas chemical content of the brine in the playa was consisted of chlorurea and sulfate (mostly chlorurea) and it was poor in carbonate and bicarbonate.

Table 1. The Petergan Playa Brines' Chemical Analysis Results Covering the Amounts of Cations and Anions and Acidity, Total Hardness and EC Levels

S.	X	Y	Cl^-	SO_4^{2-}	Na^+	Mg^{2+}	K^+	Ca^{2+}	HCO_3^-	CO_3^{2-}	TDS	EC	pH
b1	276708.5	3695554	30800	16100	30555.21	1145.41	73.48857	788.3412833	190	0.01	48.8	93	7.2
b2	278208.5	3695554	55800	9870	44297.71	1620.189	162.7152	1301.545479	100	0.01	68.9	130.2	6.9
b3	279708.5	3697054	142800	11500	108205.6	939.364	325.9846	1090.785609	80	0.01	258	489	6.9
b4	278208.5	3697054	52300	2200	36988.1	1192.897	135.4234	1709.585379	75	0.01	61.6	116	7.2
b5	276708.5	3697054	90800	19900	69964.05	554.3223	207.5392	793.4203836	95	0.02	94.3	178.4	7.4
b6	275208.5	3697054	8100	4200	7177.063	204.6725	35.61768	694.7453095	90	0.02	16	30.1	7.5
b7	273708.5	3698554	20500	18800	21021.07	1596.531	82.06211	645.3632697	235	0.01	37.5	71.2	7.4
b8	275208.5	3698554	31400	7100	23296.14	326.0734	125.522	1131.700407	85	0.01	42.5	80.1	7.4
b9	276708.5	3698554	68100	6800	48003.49	685.3318	184.3684	1569.88349	65	0.02	77.7	146.9	7
b10	278208.5	3698554	114400	4000	83182.13	2147.755	278.5121	2771.716366	45	0.01	198	375	6.3
b11	279708.5	3698554	157300	4700	108990	1578.05	234.6184	1824.031859	50	0.01	258	489	6.5
b12	281208.5	3698554	107900	4100	72474.87	3205.846	261.2399	3071.338133	55	0.02	104.3	196.9	6.6
b13	284208.5	3700054	172800	3400	114818.1	2823.17	420.0297	2195.603833	70	0.01	79.8	150.7	6.5
b14	282708.5	3700054	181300	3600	123097	3016.756	451.409	2333.858334	30	0.01	292	546	5.7
b15	281208.5	3700054	173300	4300	110593.4	3251.014	369.2936	3159.391382	40	0.01	282	532	6.3
b16	279708.5	3700054	154800	1950	92843.44	4125.001	183.3331	4730.234973	40	0.01	244	459	6
b17	278208.5	3700054	101200	2600	55593.55	4858.131	156.7486	4877.770934	50	0.02	93.2	176.3	6.4
b18	276708.5	3700054	121100	3300	75107.28	5225.753	195.352	3445.046816	50	0.01	196	375	6.5
b19	275208.5	3700054	92000	11300	66223.39	1380.435	208.6781	1195.928775	75	0.02	94.8	178.3	7.1
b20	273708.5	3700054	52400	14800	40210.8	1060.673	196.6919	917.1198863	105	0.01	64.8	122.2	7.3
b21	273708.5	3701554	23300	7600	17699.18	580.3375	95.10723	920.385229	195	0.01	34.9	65.9	7.2
b22	275208.5	3701554	80900	10800	53614.08	563.4842	117.4155	1205.116888	90	0.01	84.6	158.9	7.1
b23	276708.5	3701554	104400	10700	60891.18	584.1052	94.67508	577.5058667	50	0.01	161	266	6.8
b24	278208.5	3701554	117500	5000	73998.98	1767.571	176.656	2181.900754	75	0.02	104.5	196	6.7
b25	279708.5	3701554	133800	2700	82065.6	4632.017	257.728	4089.696378	35	0.01	215	405	6.4
b26	281208.5	3701554	144300	1500	90962.83	2105.492	227.7591	2809.149603	55	0.02	229	433	6.2
b27	282708.5	3701554	158300	2200	102541.6	4877.399	327.0944	2786.18822	55	0.01	259	476	5.8
b28	284208.5	3701554	166300	2900	111297.7	5175.117	479.7236	3260.5369	50	0.01	274	517	6
b29	285708.5	3701554	102700	4700	69879.65	2754.606	421.2496	2446.69548	75	0.01	102.5	193.8	6.5
b30	287208.5	3703054	70500	6100	52610.69	1951.428	266.0975	1669.184714	75	0.01	83.5	157.7	6.9
b31	285708.5	3703054	84000	6200	60300.87	2646.935	421.5731	2154.696488	85	0.01	84.7	159.9	6.8
b32	284208.5	3703054	120100	4400	78258.73	2517.65	372.6285	2406.897808	115	0.01	204	383	6.4

Table 1. (continued).

S.	X	Y	Cl^-	SO_4^{2-}	Na^+	Mg^{2+}	K^+	Ca^{2+}	HCO_3^-	CO_3^{2-}	TDS	EC	pH
b33	282708.5	3703054	175500	3300	106542.6	2100.484	350.2652	2182.635954	60	0.01	282	533	6
b34	281208.5	3703054	116000	3400	64941.03	2906.376	150.1993	3130.614034	70	0.02	191	358	6.3
b35	279708.5	3703054	129100	7400	59721.55	1663.116	170.9672	1246.844241	75	0.02	215	407	6.6
b36	278208.5	3703054	94900	12200	57270.46	954.9974	177.6135	898.9150852	60	0.02	97.4	183.7	6.6
b37	276708.5	3703054	63400	10200	32270.76	564.3458	109.3222	782.2169838	85	0.01	74.4	140.8	7
b38	275208.5	3703054	38300	3100	23561.93	484.3131	63.42156	806.1502633	100	0.01	50.7	96	7.2
b39	273708.5	3703054	25500	8100	16025.16	412.1189	48.51353	682.7056201	100	0.01	38.1	71.5	7.4
b42	273708.5	3704554	13500	8700	9276.477	286.9119	28.04651	568.9525865	110	0.01	24.1	45.7	7.4
b43	275208.5	3704554	15300	10100	10621.71	334.6181	39.60259	371.9828461	235	0.01	26.8	50.6	7.3
b44	276708.5	3704554	52500	15000	29192.86	525.8012	131.1045	688.0378433	110	0.01	67.7	128.3	7.2
b45	278208.5	3704554	84800	10400	43339.03	955.2786	208.72	763.2088903	85	0.01	93	174.3	6.8

b46	279708.5	3704554	114800	10000	60387.29	1372.384	254.4073	1225.429889	60	0.02	101.7	192.5	6.8
b47	281208.5	3704554	94600	3800	45876.98	2189.047	120.2002	2642.139825	55	0.02	91.8	173.7	6.8
b48	282708.5	3704554	70300	5800	35063.23	1138.099	86.03843	1832.839492	50	0.01	77.1	145.6	5.9
b49	284208.5	3704554	150000	5000	77942.43	1476.902	315.7761	1810.539861	85	0.01	241	454	6.3
b50	285708.5	3704554	98100	5800	55678.31	1581.197	258.0107	1644.788895	65	0.01	96.4	181.8	6.6
b51	287208.5	3704554	81100	3600	40506.19	2452.55	138.4093	2823.852655	90	0.01	80.9	151.7	6.7
b52	288708.5	3704554	69800	4500	37028.3	2247.051	96.30902	1919.034988	60	0.01	79.8	151	6.7
b53	290208.5	3706054	51800	8200	36003.09	2227.967	91.68178	1667.309963	160	0.01	59.8	112.3	6.8
b54	288708.5	3706054	68500	5800	46641.52	2872.356	125.2556	2238.579411	85	0.02	75.5	143	6.9
b55	287208.5	3706054	117000	3300	79615.72	3977.239	245.6594	3457.16803	120	0.01	199	377	6.7
b56	285708.5	3706054	85600	4300	60251.18	2489.787	278.4076	2925.27775	100	0.01	86.7	163.5	6.7
b57	284208.5	3706054	87900	4100	63675	1462.502	225.2976	2531.207511	70	0.01	87.5	165.4	67
b58	282708.5	3706054	136100	3400	92081.41	2930.07	265.192	3454.870707	60	0.01	227	431	6.4
b59	281208.5	3706054	177600	800	103247.8	5161.328	245.3906	9980.24525	65	0.01	291	547	6.2
b60	279708.5	3706054	76500	5400	49056.83	1923.052	213.3333	2393.793551	85	0.02	78.1	147.8	6.8
b61	278208.5	3706054	67700	10100	44482.89	1738.397	301.4872	1463.880747	70	0.02	71.2	134.5	7.2
b62	276708.5	3706054	18800	8000	15829.19	574.2303	99.85883	763.6999252	100	0.01	28.4	53.5	7.5
b63	275208.5	3706054	18800	7800	15906.44	584.8353	105.7197	1074.795919	165	0.01	28.3	53.5	7.3
b64	273708.5	3706054	133300	8400	101862.9	2480.155	267.0728	2600.60568	200	0.01	19.1	36.2	7.4
b65	273708.5	3707554	207000	1600	112052	5597.403	252.4589	7708.913027	75	0.02	16.3	31.1	7.5
b66	275208.5	3707554	45600	8100	35862.5	1032.64	201.0899	1566.426857	115	0.02	17.3	32.6	7.3

Table 1. (continued).

S.	**X**	**Y**	**Cl^-**	SO_4^{2-}	Na^+	Mg^{2+}	K^+	Ca^{2+}	HCO_3^-	CO_3^{2-}	**TDS**	**EC**	**pH**
b67	276708.5	3707554	49000	8300	36831.11	1041.718	203.7518	1444.581161	85	0.01	29.7	56.5	7.3
b68	278208.5	3707554	20700	10700	20056	1104.263	178.5991	892.6819151	75	0.01	71.4	134.3	7.1
b69	279708.5	3707554	3900	2100	3634.594	190.5127	11.19099	818.1280758	50	0.01	89	168.8	7
b70	281208.5	3707554	4200	1800	3092.72	233.8421	12.28535	716.6864739	55	0.02	87.2	164.4	6.6
b73	285708.5	3707554	4400	1600	3218.645	156.1278	10.2701	641.787902	75	0.01	76.9	144.8	7
b74	287208.5	3707554	8300	3000	6702.69	320.087	19.6424	1067.730548	55	0.01	94	177.4	6.7
b75	288708.5	3707554	64800	5000	44583.92	3371.176	110.6311	2972.745994	75	0.01	70.9	133.7	6.9
b76	290208.5	3707554	30700	5200	23532.38	1520.378	71.39703	1780.222022	130	0.02	42.9	81.2	7
b77	291708.5	3707554	33200	8800	27212.66	1814.981	78.7586	1410.240557	280	0.02	46.1	86.1	7
b78	291708.5	3709054	12200	4100	9721.213	728.247	30.1328	1393.400359	255	0.01	19.9	37.7	7.2
b79	290208.5	3709054	55000	9600	44761.85	2567.435	87.19047	1502.959299	115	0.01	67.8	127.9	7.1
b80	288708.5	3709054	87700	4100	63244.2	4014.085	190.2929	3465.860254	55	0.01	91.5	172.7	6.9
b81	287208.5	3709054	117500	2800	87949.64	3985.175	265.892	4127.332685	55	0.01	219	416	6.6
b82	285708.5	3709054	87400	7800	66188.16	2112.127	271.3973	1815.179484	80	0.01	91.6	171.2	6.9
b83	284208.5	3709054	141700	8100	101481.4	1762.185	280.5705	1493.304182	60	0.01	236	445	6.8
b84	282708.5	3709054	147900	5600	106118.4	2253.011	223.5339	2030.940108	75	0.01	252	474	6.6
b85	281208.5	3709054	126500	2400	91961.61	4261.012	243.8905	4217.006966	75	0.01	232	438	6.5
b86	279708.5	3709054	65100	4100	46403.45	2819.313	173.7411	2446.000815	60	0.01	71.5	135.3	7
b87	278208.5	3709054	74600	8100	5267	127	29	143	65	0.01	84.5	157.9	7.1
b88	276708.5	3709054	19900	7100	15458.09	1213.406	138.0145	1075.872165	125	0.01	30.3	57.4	7.4
b89	275208.5	3709054	11400	4600	12502.99	738.8229	93.90672	1020.52317	135	0.01	25	471	7.4
b94	276708.5	3710554	29100	8700	21912.39	1217.846	190.5845	1164.390316	115	0.01	41.7	78.6	7.5
b95	278208.5	3710554	44300	7600	34974.12	1181.244	215.0344	1381.866637	90	0.01	60.4	114.2	7.4

b96	279708.5	3710554	144900	5600	98648.81	2406.297	247.6648	2455.798925	50	0.01	230	434	6.4
b97	281208.5	3710554	189000	1400	104114.8	5190.164	230.2671	6988.155629	40	0.01	281	532	6
b103	279708.5	3712054	49100	8400	33220.27	939.3824	180.2452	1321.312342	90	0.01	59.9	113	7.3
b104	278208.5	3712054	50300	8600	24395.17	599.4978	116.1809	917.1794501	85	0.01	61	114.9	7.3
b105	276708.5	3712054	24800	12600	18195.05	978.514	148.8175	889.3431176	285	0.01	38.5	72.9	7.8
sp1	281424	3696764	4200	2200	3509.092	183.0237	8.888868	770.7240909	225	0.01	8.06	15.2	8
sp2	281304.5	3696292	4200	2000	2943.962	221.5241	6.804509	666.8034167	180	0.01	7.54	14.27	7
sp3	281133	3695639	20400	6100	13983.24	752.5803	50.69577	1157.937284	495	0.02	29.9	56.3	7.1
sp4	281731.9	3695280	33600	10300	22572.74	1170.373	129.553	1097.652432	275	0.02	47.5	89.7	6.3
sp5	281814.1	3695378	4700	2000	3218.616	154.4115	7.135308	630.6234222	175	0.02	8.87	16.72	7.7
sp6	281831.6	3695544	8700	3100	5425.24	255.5277	11.12612	837.0545914	225	0.01	14.6	27.6	7.7
sp7	282086.4	3696345	1900	900	1323.163	144.2494	9.497303	259.9765409	125	0.01	4.01	7.57	7.4
sp8	289664.1	3703233	23700	6500	14336.56	563.1955	42.20627	1057.509506	365	0.01	33.9	64	7.2

As illustrated in Fig. 7, in spite of the ingress waters of variegated contents, chemical combination of brines rests solely on one apex of triangle, so that it rests on the anions' 3 lateral diagram contiguous to the Cl^-, SO_4^{2-} side and on the cations' diagram, contiguous to the Na^++ Cl^- side. Therefore, the brine´s chemical content was as follows: Na^+ – Cl^- – SO_4^{2-}. Even though, concentration of anions and cations measured in brines in different areas was more or less dissimilar to one another, chemical content could be stable and even can be pondered with respect to foregoing kind in terms of abundance. Altogether, by pondering about the Piper diagram, it can be said that, chemical content of the brines falls within Na^+ and K^+ realm denoting the non–carbonate brines.

Moreover, the data obtained on the nature of ingress waters (both surface and subterranean) from the database of the Southern Khorasan Province Water Authority showed that, surface waters bear less calcium and magnesium and further sulfate and bicarbonate compared to the brines and hydro geochemically, they are of Ca^{2+}– Na^+– Cl^- type. Additionally, subterranean waters (wells and qanats) bear further Mg and bicarbonate, and hydrogeochemically they are of Ca^{2+}– Na^+– Cl^- type.

Chemical data of brines were investigated using the Stiff diagram, aimed at distinguishing the evaporate salts incorporated in the brines. The Stiff diagrams (Fig. 8) displaying average concentration of salts probably found in the brines are represented in Fig. 8. The Na^+ and K^+ cations, as illustrated in foregoing diagram, show the highest level of correlation and association with Cl^- anions ,according to which it can be concluded that, the likelihood of presence of NaCl (Halite) and KCl (Sylvite) is significantly high. The next strong correlation belonged to Ca^{2+} and carbonate and bicarbonate, and abundance of CaCO3 salts (Calcite) was found to be high in the brines. Ultimately, it can be said that, there is a correlation between Mg^{2+} and sulfate with a high likelihood of $MgSO_4$ (Epsomite) in the brines.

Discussion

Evolution of brines may be associated with kind of outcrops, reaction with existing waters, and characteristics of waters (Jones & Deocampo, 2003, 2014). Rock type of the outcrops can influence on evolution of the brines and the amount of cations and anions. Solubility varies in different types of rock; this would instigate lack of balance/ discrepancy in initial ratio of $HCO_3^-/Ca^{2+}+ Mg^{2+}$ in solution, as revealed by pondering about an overarching control in evolutionary trend of the brine (Jones & Deocampo, 2003). The analogy of Stiff diagram depicted for the principle brines with waters joining surface and subterranean peers around the basin manifests a significant rise in concentration of anions and cations towards the center (analogy of Fig. 8); the control responsible for such shifts may result from the kind of rocks forming the outcrops around the basin and evolution of brines.

So, first, the characteristics of the outcrops around the basin were discussed followed by evaluating the results obtained on evolution of brines. The rocks forming the watershed are of different types including evaporites, pyroclastics, carbonates, mafic silicates, plagioclase feldspars, calcites–sulphides, and silicate sulphides.

Considering the outcrops, lithologic units are spread mostly in the vicinity of silicates and sulphides which have also influenced chemical composition of waters $Ca^{2+} + Mg^{2+} > CO_3^{2-}$. This is while, distribution of the pyroclastics is less (%) creating a chemical composition of $CO_3^{2-} \gg Ca^{2+} > Mg^{2+}$.

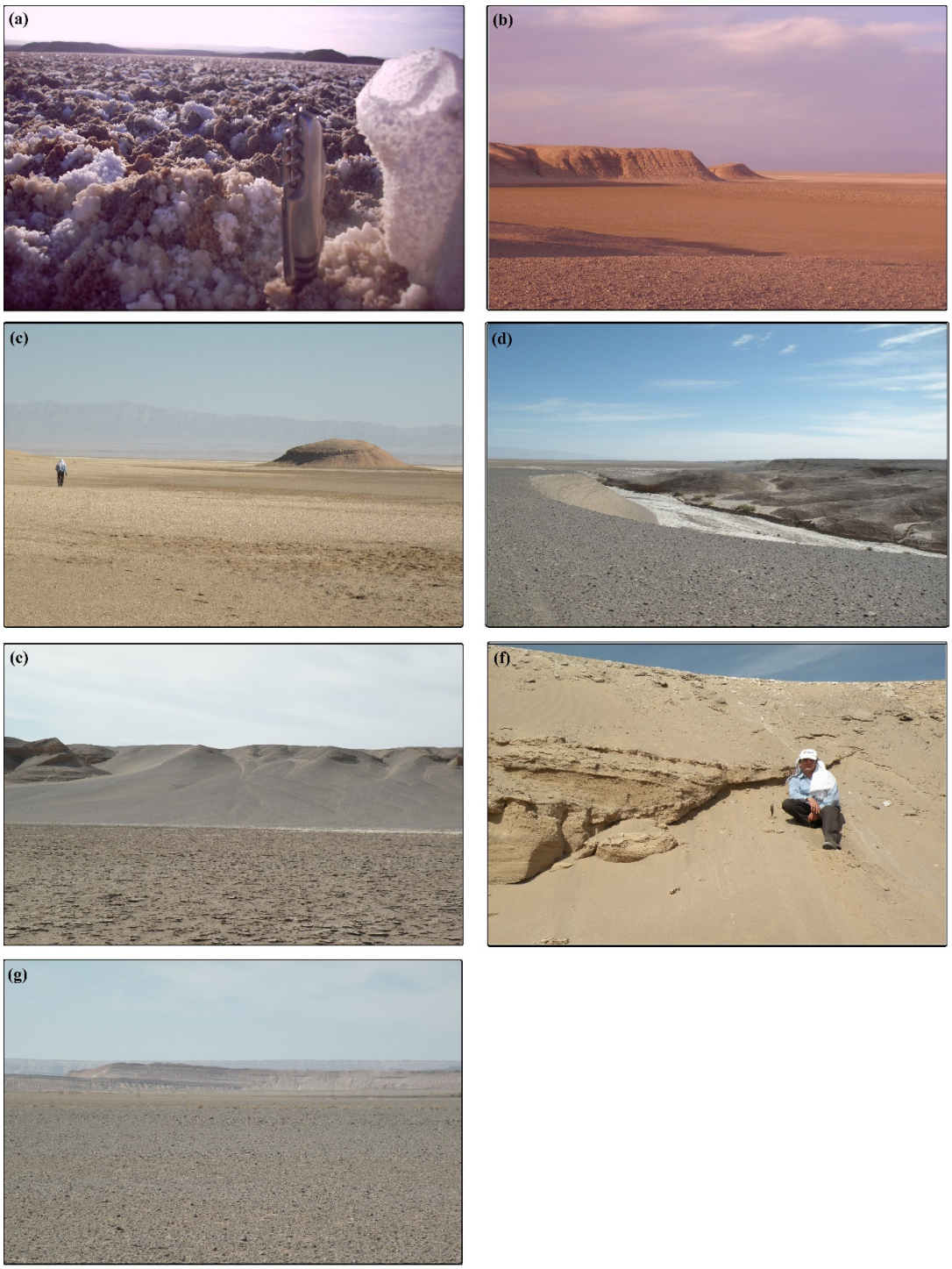

Figure 6. (a) Desert sediments and sedimentary rocks (front view) and western igneous rocks (bottom view) (To view the image to the west). (b,c) Sandstone, clay, shale, and conglomerate with red cement and iron in the Lower Cretaceous (To view the image to the north). (d, e, f) Depositional alluvium, salt, muddy, and sandy flats, as well as running sands (To view the image to the northeast). (g) Carbonate rocks (Limestone and dolomite) in the study area (To view the image to the south).

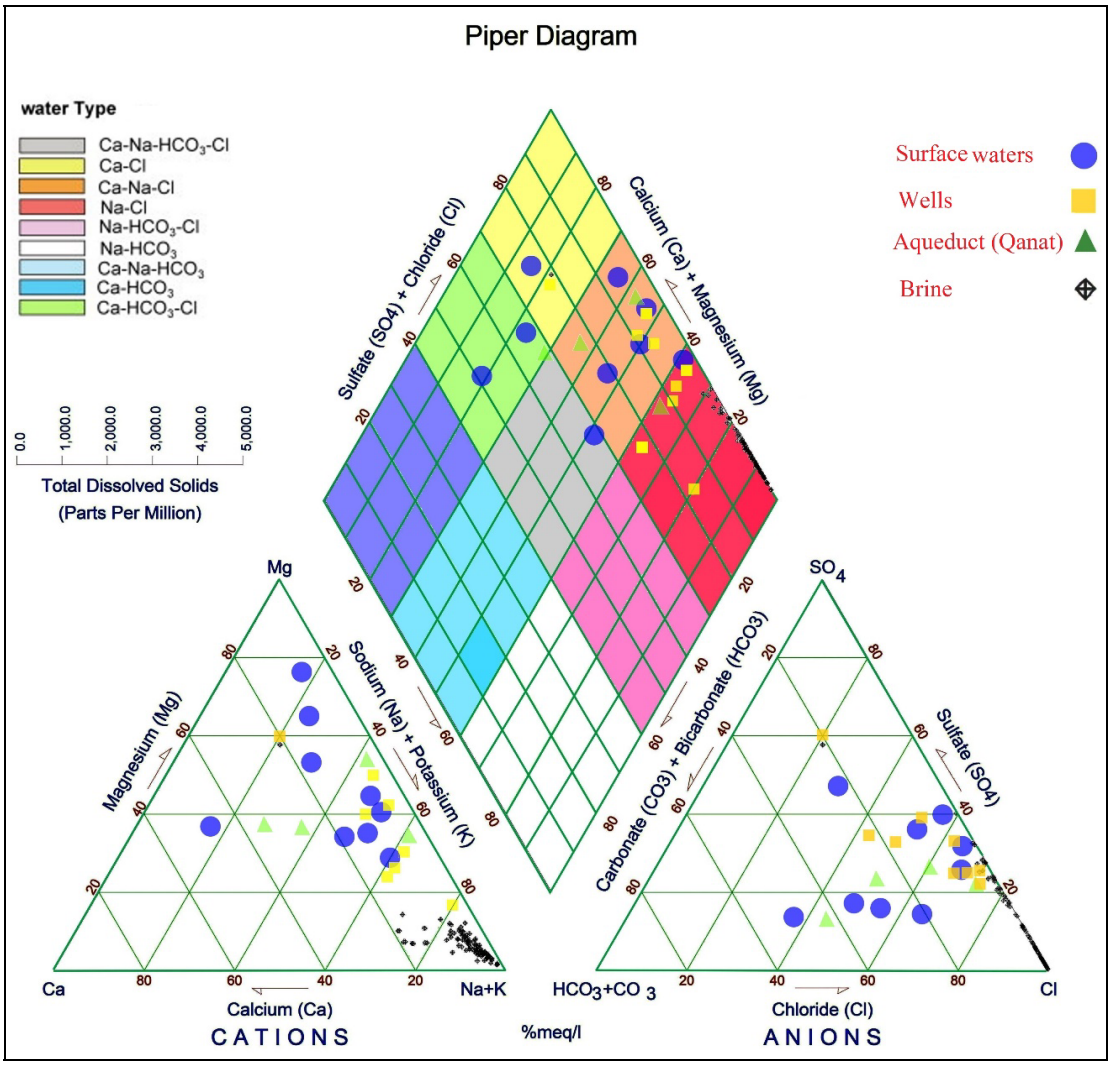

Figure 7. Piper diagram depicted for the entire subterranean waters and the brines in the Petergan Playa.

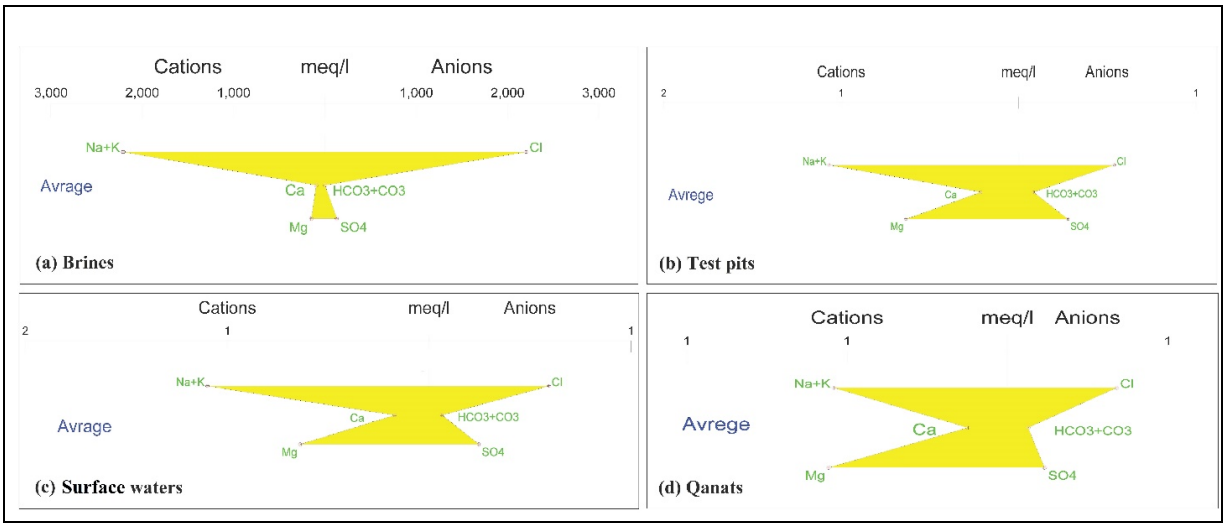

Figure 8. Stiff diagram depicted for the principle contents of the Petergan Playa (a) brines, (b) test pits, (c) surface waters & (d) qanats.

Results of analysis on ingress waters (qanats, wells, and surface waters) and the brines (see Tables 1, 2, 3, and 4) showed that, ratio of Ca^{2+} and Mg^{2+} is higher than that of carbonate and bicarbonate, which $Ca^{2+} > CO_3^{2-}, Cl^- + SO_4^{2-} > HCO_3^-, Ca^{2+} + Mg^{2+} > CO_3^{2-}$ molar ratios can be considered as chemical composition at ingress waters, based on the classification chart proposed by Jones & Deocampo (2014) (see also Fig. 9). Therefore, dissolution of evaporates, dissolution and oxidation of calcite and sulphides, and oxidation and weathering of silicates and sulphides caused the most remarkable effect on chemical content of the brines. Seemingly, 81% of the outcrops would have been formed by foregoing units based on the zonation and lithological description (Figs. 4 and 5) of which silicates, evaporates, calcite, and sulphides have been cropped out by 79, 1.6, and 0.4% in the area.

The processes contribute in evolution of the ingress waters into concentrated brines are unabated evaporation, recycling of formerly developed minerals simultaneously with deposition, diagenetic reactions, exchange of pore fluids, the reduction of sulphate, and exchange of ion (Drever & Smit, 1978; Hardie *et al.,* 1978). Deposition of moderately insoluble initial minerals such as earth alkali carbonates (low –Mg calcite, high –Mg calcite, and aragonite) and gypsum is a fundamental stage by which the brine evolution is controlled (Hardie & Eugster, 1970).

Hardie & Eugster (1978) in their extensive investigations on evolution of brines declared that ,there are three disparate routes influencing on evolutional chemical upheavals of water in confined basins that contribute in introduction of the ultimate brine as routes I, Π ,and Ш (see Fig. 10).

Table 2. Average Amount of Ions Measured in the Qanats in Shahrakht–Petergan Playa Based on ppm in 2015.

Location	X	Y	Cl^-	SO_4^{2-}	Na^+	Mg^{2+}	K^+	Ca^{2+}	HCO_3^-	CO_3^{2-}	pH	TDS	EC
Hajiabad	777606	3722660	33.3	13.5	29.8	19.5	0.06	3.8	5.5	0.02	7.53	3421.8	5360
Shahrakht	247238	3724672	10	6.3	14.1	3.9	0.02	1.5	3.4	0.01	7.12	1265.4	1990
Mohammadabad	232283	3706704	3.3	1.4	3.7	2.6	0.01	3.5	5.2	0.01	7.16	629.5	1008
Abiz	772890	3731453	1.7	1	2.1	1.1	0.01	1.2	1.6	0.03	7.45	290.5	458

Table 3. Average Amount of Ions Measured in the Test pits in the Shahrakht–Petergan Playa Based on ppm in 2015.

Location	X	Y	Cl^-	SO_4^{2-}	Na^+	Mg^{2+}	K^+	Ca^{2+}	HCO_3^-	CO_3^{2-}	pH	TDS	EC
Shahrakht	251373	3718586	22.1	10.1	25.9	5.6	0.04	4.6	3.3	0.01	7.02	2365.5	3710
Barenjegan	257090	3716857	32	18.5	35.2	14.3	0.05	3.7	3.5	0.02	7.32	3611.2	5660
Chah–e Zard	260072	3707694	7.1	7	14.8	3.6	0.02	1.5	6	0.03	6.98	1351.8	2140
Shahrakht	243972	3724142	14.8	14.6	23.1	5	0.04	4	3.7	0.01	7.2	2200	3440
Shahrakht	242933	3723279	30.1	13.5	33	7.5	0.05	5.1	2.8	0.01	7.04	3021.9	4750
Barenjegan	255738	3717705	33.1	15.1	31	16.3	0.05	3.8	3.8	0.01	7.27	3374.2	5290
Bamrud	232818	3724668	19.8	8.1	19	7.9	0.05	3.6	2.8	0.03	6.81	2004.5	3150
Masumabad	263799	3709191	9.2	8.1	19.8	1.9	0.04	1.1	5.7	0.03	7.63	1515.4	2390

Table 4. Average Amount of Ions Measured in the Rivers/surface waters in the Shahrakht–Petergan Playa Based on ppm in 2016.

S.	X	Y	Cl^-	SO_4^{2-}	Na^+	Mg^{2+}	K^+	Ca^{2+}	HCO_3^-	CO_3^{2-}	pH	TDS	Ec
1	60.14	33.38	7.4	12.9	17	4	0.02	2.5	2.5	0.01	8.19	1550	2440
2	59.75	33.52778	24	13	25.6	8.5	0.05	4.8	4.1	0.01	7.63	2750	4300
3	60.72	31.39944	44	40	58	14.9	0.12	13.4	3.1	0.03	7.81	5670	8890
4	56.97	33.81611	6.2	2.5	4.3	8	0.01	1.8	5.6	0.01	6.54	915	1443
5	59.82	32.24333	1.5	3	2	1.7	0.01	3.2	2	0.01	7.23	440	693
6	57.13	33.65306	4.9	4.4	4.9	3.9	0.01	2.1	1.1	0.01	7.61	700	1109
7	56.87	33.825	14.1	4.8	18	6.8	0.03	1.9	8.2	0.01	6.77	1740	2730
8	57.27	33.465	3.1	1.5	3.5	6.5	0.01	1.1	6.8	0.01	7.07	730	1150
9	59.34	33.78639	74.6	45	90	18.6	0.15	10.9	4	0.02	7.94	8020	12540
10	59.64	33.05111	11	5.5	23	4.6	0.03	1.5	12.4	0.01	7.69	1890	2970

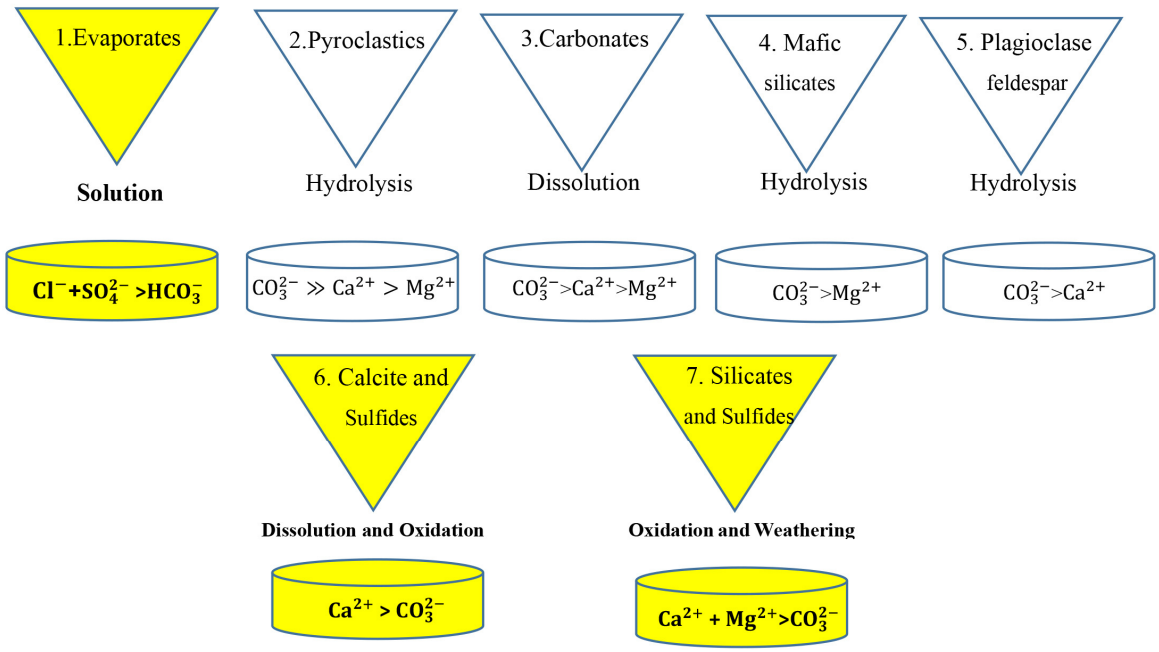

Figure 9. The relationship between the origin and combination of brines after Jones & Deocampo (2003).

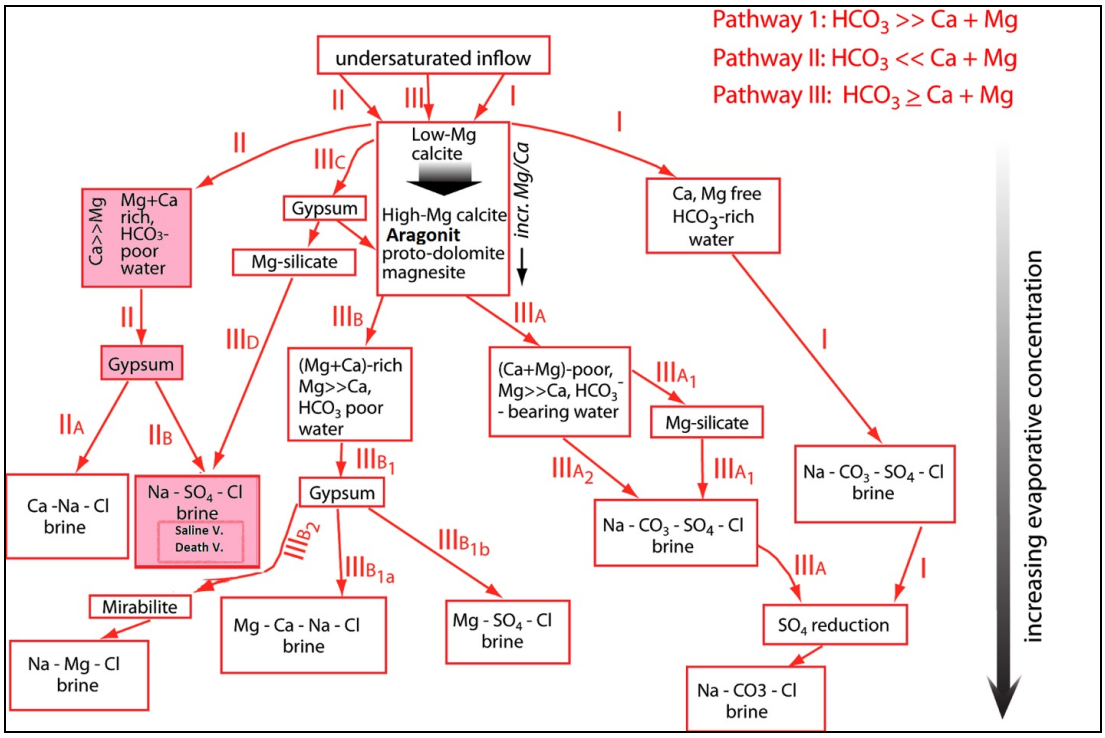

Figure 10. Brine evolution diagram (dashed lines symbolise the evolutionary route of brines in the Petergan Playa) (Hardie & Eugester, 1978; Warren, 2010).

Evolutionary route I is a signature to the ingress waters of low Ca^{2+} and Mg^{2+} ions for the alkali brine. The content of ingress waters is dependent on extremely high molar ratio basins of $HCO_3^-/Ca^{2+} + Mg^{2+}$, $(HCO_3^- \gg Ca^{2+} + Mg^{2+})$. The waters would cause deposition of earth alkali carbonates in depositional basins, forming alkali brines rich in $SO_4^{2-}, CO_3^{2-}, HCO_3^-, K^+, Na^+$ and Cl^-

(Surdam & Eugester, 1976; Warren, 2006). Along the revolutionary route II, initial ingress waters are poor in bicarbonate ions and their molar ratio are extremely low $(HCO_3^- \ll Ca^{2+} + Mg^{2+})HCO_3^-/Ca^{2+} + Mg^{2+}$, indicating that resulting brine would be of chlorurea or sulfate type (Fayazi, 1991; Lak, 2016). Ultimately, at the end of evolutionary route III, none of the ions of $(HCO_3^-, Ca^{2+}, Mg^{2+}, HCO_3^- \geq Ca^{2+} + Mg^{2+})$ found in ingress waters is dominant. The ingress waters contain the following ion combination of $HCO_3^- \geq Ca^{2+} + Mg^{2+}$. This stage contributes in development of the brines of Na^+– CO_3^{2-}- SO_4^{2-}, Na^+– Mg^{2+}– Cl^- (Lak, 2007), Mg^{2+}– Ca^{2+}– Na^+– Cl^- or the brines of Mg^{2+}- SO_4^{2-}- Cl^- (Hardie & Eugester, 1970).

Regarding geochemical trend for evolution of the brines, ingress waters (waters introduced into the basin) are chiefly composed of silicate and sulphides, evaporate and calaite, calcite, and sulphide. They possess molar ratios of Ca^{2+} + $Mg^{2+} > CO_3^{2-}$, $Ca^{2+} > CO_3^{2-}$, $Cl^- + SO_4^{2-} > HCO_3^-$, so that the combination of $HCO_3^-/Ca^{2+} + Mg^{2+}$ can be considered as chemical composition of waters introduced into Petergan Playa. Considering Fig. 10, therefore, the route Π indicates evolutionary trend of the playa. The bicarbonates are swiftly dissolved, along the route meanwhile the alkali soils get rich in alkaline material. Possibly, the waters, never develop Mg^{2+}–rich carbonates due to swift loss of bicarbonates; therefore, deposition of calcite occurs followed by deposition of gypsum. If sulfate ion overcomes the earth alkali elements, a brine of Na^+– SO_4^{2-}– Cl^- would form. Samples were analyzed using the XRD in order to determine mineralogical characteristics of soil. Given the data presented in Fig. 11, it can be estimated that, gypsum ($CaSO_4 2H_2O$) is the most abundant evaporite mineral in the playa, confirming evolutionary trend of the brine in/through route Π. A replica of such brines does exist in the Saline Valley and the Dead Valley Playas. Another instance is the Meyghan Playa possessing extremely low content of bicarbonate $HCO_3^- \ll Ca^{2+} + Mg^{2+}$ that follows the route Π. The playa brines assessed in the study area showed similar characteristics to those in the regional scale in Kuwait (Ahmed *et al.,* 2014).

Conclusion

In the present research, to study the Petergan Playa lying in northeast of Iran, sampling was conducted from some of 95 brines, and ICP–MS results indicated that , chemical combination of the brine is composed of chlorurea and sulfate (mostly chlorurea) and is poor in carbonate and bicarbonate, forming a brine of Na^+– Cl^-– SO_4^{2-} type.

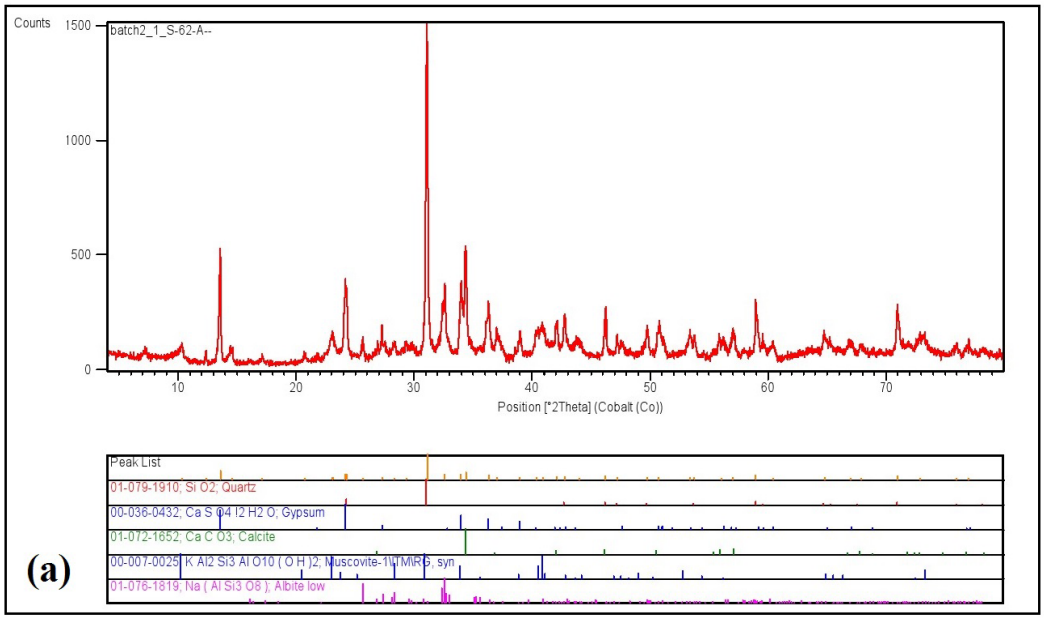

Figure 11. The XRD diagrams of the brines of the Petergan Playa: (a) Quartz, Gypsum, Clacite, Muscovite, Albite; (b) Quartz, Gypsum, Halite, Clacite, Muscovite, Clinochlore.

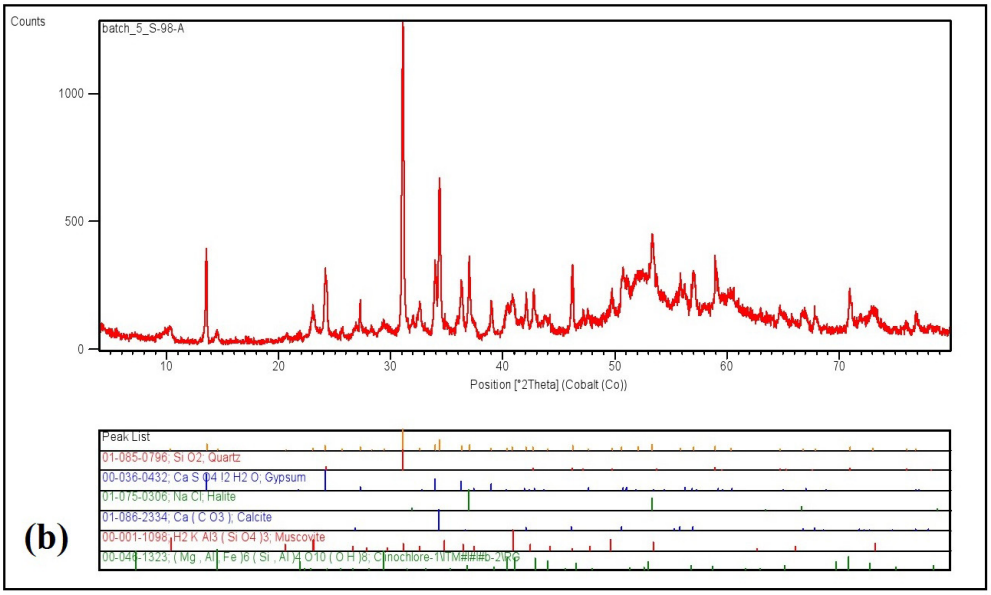

Figure 11. To be continued.

Results of studying physio–chemical parameters showed that, average acidity measured in the brines is equal to 6.9 indicating neutral to slightly alkaline, EC of brines was equal to 159.4 mS/cm on average, rate of total hardness was equal to 84.5 mg/L, and quality hardness of the waters was medium light.

Based on analyses performed on ingress waters (qanats, wells, and surface waters), amount of Ca^{2+} and Mg^{2+} was found to be high in the Petergan Playa compared to carbonate and bicarbonate. Molar ratios in ingress waters were as follows: $Ca^{2+}>CO_3^{2-}$, $Cl^{-}+SO_4^{2-}>HCO_3^{-}$, $Ca^{2+}+Mg^{2+}>CO_3^{2-}$. According to the classification proposed by Jones & Deocampo (2014), it can be concluded that, dissolution of evaporates, dissolution and oxidation of calcite and sulphides, and oxidation and weathering of silicates and sulphides have had the most noticeable effects on chemical combination of the brines. Evolutionary route of the brines as presented on the diagram in the study by Hardie and Eugester has been poor in bicarbonate ion and low in molar ratio ($HCO_3^{-} \ll Ca^{2+} + Mg^{2+}$) $HCO_3^{-}/Ca^{2+}+ Mg^{2+}$which has resulted in a chlorurea or sulfate type of brine complying with the route Π, which its evolutionary route resembles the American counterparts of Saline and Dead Valleys. It is highly recommended to use native plants for rehabilitation in the study area (Al–Dousari *et al.,* 2018)

Acknowledgments

We would like to thank all the individuals who contributed in this research project. In particular, we appreciate the manager of Ministry of Industry, Mine, and Trade, Iranian Mines and Mining Industries Development and Renovation Organization (*IMIDRO*), and Pars Pey Azma Company for provision of some data and information.

References

Aba, A., Al–Dousari, A. M., Ismaeel, A., 2016. Depositional characteristics of 7 Be and 210 Pb in Kuwaiti dust. Journal of Radioanalytical and Nuclear Chemistry, 307(1): 15–23.

Aba, A., Al–Dousari, A. M., Ismaeel, A., 2018. Atmospheric deposition fluxes of 137Cs associated with dust fallout in the northeastern Arabian Gulf. Journal of environmental radioactivity, 192: 565–572.

Ahmed, M., Al–Dousari N. and Al–Dousari A., 2014. Rehabilitation of Degraded Lands Using Environmentally Friendly Techniques. International Symposium on Native Plant Production" 10–13 Nov, Kuwait Institute for Scientific Research, Kuwait.

Ahmed M., Al–Dousari N., Al–Dousari A., 2016. The role of dominant perennial native plant species in controlling the mobile sand encroachment and fallen dust problem in Kuwait. Arabian Journal of Geosciences: 12112.

Al–Dousari, A. M., 2005. Causes and Indicators of Land Degradation in the North–Western Part of Kuwait. Arab Gulf

Journal of Scientific Research (1989), 23(2): 69–79.
Al–Dousari, A. M., & Al–Hazza, A., 2013. Physical properties of aeolian sediments within major dune corridor in Kuwait. Arabian Journal of Geosciences, 6(2): 519–527.
Al–Dousari AM, Ibrahim M.I, Al–Dousari N, Ahmed M, Al–Awadhi S., 2018. Environmental and economic importance of native plants and green belts in controlling mobile sand and dust hazards. International Journal of Environmental Science and Technology. DOI:10.1007/s13762–018–1879–4.
Al–Dousari, A. M., 2009. Recent studies on dust fallout within preserved and open areas in Kuwait. Bhat NR Al–Nasser A, Omar S (eds) Desertification in arid lands. Institute for Scientific Research, Kuwait, 137–147.
Al–Dousari, A. M., Aba, A., Al–Awadhi, S., Ahmed, M., & Al–Dousari, N., 2016. Temporal and spatial assessment of pollen, radionuclides, minerals and trace elements in deposited dust within Kuwait. Arabian Journal of Geosciences, 9(2): 95.
Abdi, L. and RahimpourBonaab, H., 2010. Origin of hydrogeochemical and evolution of brine in Playa Mighan. research and sedimentology stratigraphy, age 26, 38(I): 42–25. (in Persian)
Bahadori, A., Garranza, E. J. M. and Soleimani, B., 2011. Geochemical analysis of evaporite sedimentation in the Gachsaran formation, Zeloi oil field, southwest of Iran. Journal of Geochemical Exploration, 111(3): 97–112.
Drever, J. I. and Smith, C. L., 1978. Cyclic wetting and drying of the soil zone as an influence on the chemistry of ground water in arid terrains. American Journal of Science, 278(10): 1448–1454.
Eugster, H. P. and Hardie, L. A., 1978. Saline lakes. In A. Lerman (Ed.), Lakes, chemistry, geology, and physics (pp. 237–293). New York, NY: Springer Verlag.
Fauvelet, E. and Eftekhar Nezhad, J., 1990. Geological report of Shahrakht map. Tehran: Geological Survey of Iran, Scale1:250000.
Fayazi, F., Lak, R. and Nakhaei, M., 2007. Hydrogeochemistry and brine evolution of Maharlou Saline Lake, southwest of Iran. Carbonates and Evaporites, 22(1): 34–42.
Hardie, L. A., 1968. The origin of the recent non marine evaporate deposit of Saline Valley, Inyo County, California. Geochemica et Cosmochemica Acta, 32(12: 1279–1301.
Hardie, L. A. and Eugester, H. P., 1970. The evolution of Closed basin brines. Mineralogical Society of America, 3: 273–290.
Hardie, L. A. and Eugester. H. P., 1978. Saline lakes. In A. Lerman (Ed.), Lakes: Chemistry, geology, physics (pp. 237–293). New York, NY: Springer–Verlag.
Hardie, L. A., Smoot, J. P. and Eugester, H. P., 1978. Saline lakes and their deposits: A sedimentological approach. In A. Matter & M. E. Tucker (Eds.), Modern and ancient lake sediments (pp. 7–42). New Jersey, NJ: John Wiley & Sons.
Jones, B. F. and Deocampo, D. M., 2003. Geochemistry of saline lakes. Treatise on Geochemistry, 5: 393–424.
Jones, B., F. and Deocampo, D. M., 2014. Geochemistry of saline lakes. Treatise on Geochemistry, 7: 437–469.
Krinsley, D. B., 1970. Geomorphological and paleoclimatological studies of the Playa of Iran. Washington, DC: US Government Printing Office.
Lak, R., 2007. Sedimentology and hydrogeochemistry characteristics and evolution process of brines of Howz–e–Soltan Lake in Qom. Quaternary Journal of Iran, 2(1): 79–91.
Lak, R., 2007. Investigation of sedimentology, hydrochemistry and brine evolution trend of Maharlou Lake (Unpublished doctoral dissertation). Kharazmi University, Tehran, Iran. (in Persian)
Lak, R., 2016. The hydrogeochemistry characteristics and determined the source and evolution of brines of the Lake Maharlou (Unpublished doctoral dissertation). Tarbiat Moallem University, Tehran, Iran. (in Persian)
Li, M., Fang, X., Wang Song, Y., Yang, Y., Zhang, W. and Liu, X., 2013. Evaporite minerals of the lower 538.5 m sediments in a long core from the Western Qaidam Basin, Tibet. Quaternary International, 298: 123–133.
Ma, L., Lowenstein, K. T., Li, B., Jiang, P., Liu Ch., Zhong J., Wu, H., 2010. Hydrochemical characteristics and brine evolution paths of Lop nor Basin, Xinjiang Province, Western China. Applied Geochemistry, 25(11): 1770–1782.
Mahajerani, Sh., 1999. Sedimantologyof Mighan desert with special approach on the origin and developing of evaporative depositions (unpublished master's thesis). University of Tehran, Tehran, Iran. (in Persian)
Sa'deddin, N., 2006. Systematic geochemical studies of 1:100000 of Shahrakht and Yazdaan. Geological Survey of Iran, 3: 5–6. (in Persian)
Surdam, R. C. and Eugster, H. P., 1676. Mineral reaction in sedimentary deposits of Lake Magadi region, Kenya. Geological Society of America Bulletin, 87: 1739–1752.
Torshizian H. and MusaviHarami, R., 1999. The sedimentology, geochemistry and hydrogeochemistry phenomena of Zarrin Playa in Central Iran. Iranian Journal of Earth Science, 29(30): 16–21. (in Persian)
Torshizian, H. and Mollai, H., 2006, November. Hydrochemstrical analysis of Siyah–Kuh playa brines in central Iran. Paper presented at the 6th International Conference on the Geological of the Middle East, Al Ain, Emirates.
Torshizian, H., 2009. Evolution of Brine and formation evaporative minerals in Saghand Playa in central Iran, and compare with great Salt Lake and Death Valley basin in the US. Iranian Journal of Crystallography and Mineralogy,

17(1): 43–54. (in Persian)
Warren, J., 2006. Evaporates: Sediment, resources and hydrocarbons. Berlin, Germany: Springer.
Warren, J., 2010. Evaporites through time: Tectonic, climatic and eustatic controls in marine and non–marine deposits. Journal of Earth–Science Reviews, 98(3–4): 217–267.
Williams, V., 2005. Afghanistan geological survey: Geologic Map of Quadrangles 3460 and 3360, Kol–I–Namaksar (407), Ghuryan (408), Kavir–I–Naizar (413), and Kohe–Mahmudo–Esmailjan (414) Quadrangles, Afghanistan. Reston, VA: The United States Geological Survey (USGS), Scale 1:250000.